Preprint
UCRL-JC-150767

Direct Observation of Stimulated Brillouin Scattering (SBS) Detuning by a Velocity Gradient

D.H. Foula, L. Divol, A. MacKinnon, G. Gregori, and S.H. Glenzer

This article was submitted to Physics Review Letters

September 25, 2002

U.S. Department of Energy

Lawrence
Livermore
National
Laboratory

UCRL-WEB-146893 Rev1-v4no1-03

Direct observation of stimulated Brillouin scattering (SBS) detuning by a velocity gradient

D. H. Froula,* L. Divol, A. MacKinnon, G. Gregori, and S. H. Glenzer
L-399, Lawrence Livermore National Laboratory
University of California P. O. Box 808, CA 94551, U.S.A.

We report the first direct evidence of detuning of stimulated Brillouin scattering (SBS) by a velocity gradient, which was achieved by directly measuring the frequency shift of the SBS driven acoustic wave relative to the local resonant acoustic frequency. We show that in the expanding part of the plasma, ion-acoustic waves are driven off-resonance which leads to the saturation of the SBS instability. These measurements are well reproduced by fluid simulations that include the measured flow.

PACS numbers: 52.25.Qt, 52.35.Fp, 52.40.Nk, 52.50.Jm

Stimulated Brillouin scattering (SBS) is a result the resonant ponderomotive coupling of an incident light wave, a reflected light wave, and an ion-acoustic wave. This resonance can drive ion-acoustic waves to large amplitudes. In principle, this process could result in the reflection of a large fraction of the incident energy for inertial confinement fusion (ICF) targets. In order to minimize this energy loss, a good understanding of mechanisms that could limit SBS is important. In many targets, the velocity gradient within the expanding plasma provides such a mechanism; the frequency of the local acoustic waves is Doppler shifted, therefore, detuning the three-wave resonant process [1].

In this letter, we present the first direct measurement of SBS detuning by a velocity gradient. A novel use of two Thomson-scattering diagnostics has allowed us to directly measure the frequency and amplitude of the ion-acoustic wave responsible for SBS as a function of space. This is the first measurement that spatially resolves both the frequency and the amplitude of the ion-acoustic waves directly responsible for SBS. These measurements link the saturation of the SBS instability to the frequency detuning from an expanding plasma. We have independently measured the ion-acoustic frequency and the frequency of the driven acoustic wave at various positions in the plasma. Therefore, by comparing the local ion-acoustic frequency, with the local frequency of the driven acoustic wave we have measured the actual detuning of the SBS instability. The measured electron temperature, velocity gradient, and electron density have been included in fluid simulations which clearly support the measured SBS detuning by a velocity gradient.

The experiments used a three-beam configuration at the Trident Laser Facility [2]. The Be plasmas were produced by a heater beam with 180 J of 2ω ($\lambda = 527$ nm) laser light in a 1.2-ns-long square pulse. The heater beam was focused normal to the target surface using an $f/6$ lens and a strip line random phase plate (Fig. 1c). This produced a line focus with an intensity of 10^{14} W cm^{-2} and an initial 1000 μm $\times$ 100 μm Be plasma [3]. An interaction beam (50 J, 2ω, 1.2-ns-long square pulse) was

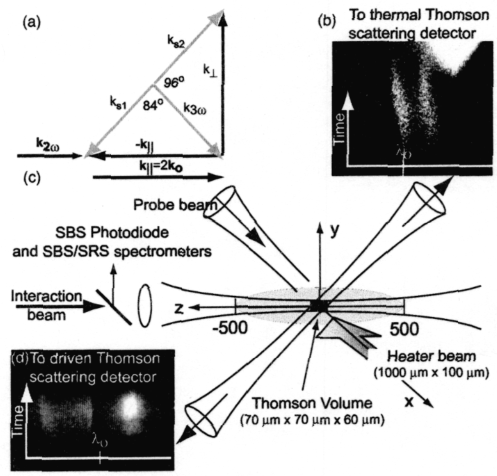

FIG. 1: (a) A diagram detailing the ion-acoustic wave-vectors probed is shown in the top left corner. (b) A thermal Thomson-scattering spectrum ($k_\perp$) and (d) a driven Thomson-scattering spectrum ($k_{||}$) are shown. (c) The experimental setup is shown.

aligned x= 400 μm from the target surface and was focused to a 60 μm diameter spot, resulting in an intensity of 1.5×10^{15} W cm^{-2}. The interaction beam was used to drive SBS which excites ion-acoustic waves with wave-vector $\mathbf{k}_{||} = 2\mathbf{k_o}$ co-propagating in the direction of the interaction beam. The backscattered SBS light was collected and collimated by the focusing lens of the interaction beam. A fraction of the backscattered light was focused on to a fast photodiode and two, 1/4-meter SRS and 1-meter SBS, spectrometers. The SRS and SBS spectra were measured with a respective resolution of 0.5 nm and 0.45 Å. The absolute SBS energy was measured with the diode [4].

The third laser beam, 3ω ($\lambda = 351$ nm), was used as a Thomson probe beam. The probe beam and Thomson-scattering collection optics define a volume (70 μm$\times$70 μm$\times$60 μm) located at the center of the chamber. Light scattered from the Thomson-scattering volume was imaged onto two separate Thomson-

UCRL-WEB-146893 Rev1-v4no1-03

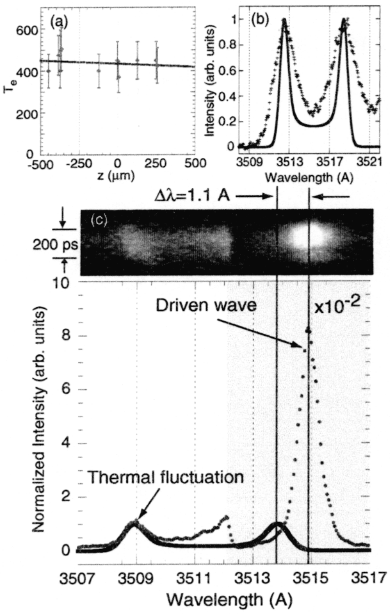

FIG. 2: (a) A constant electron temperature, $T_e = 450$ eV, is measured along the interaction beam axis. (b) Representative Thomson-scattering spectra taken from the spectra in Fig. 1b where light is scattered from ion-acoustic fluctuations propagating perpendicular to the interaction beam ($\mathbf{k}_\perp$). (c) Thomson-scattering data are shown collected by the diagnostic observing ion-acoustic waves propagating parallel to the interaction beam ($\mathbf{k}_{||}$). The spectra (points) is shown below averaged over 50 ps. The theoretical form factor (solid line) is fit to the blue-shifted light using a velocity flow $\frac{v}{v_{th}} = 0.7$ and the electron temperature measured with the first Thomson-scattering diagnostic ($T_e = 450$ eV). The shaded region was optically filtered by x100.

scattering spectrometers. The interaction beam is focused in the middle of this volume. The first Thomson-scattering diagnostic probes ion-acoustic fluctuations (Fig. 1b) propagating perpendicular to the interaction beam ($\mathbf{k} = \mathbf{k}_\perp$) and allows us to independently measure the electron temperature T_e. The geometry (Fig. 1a) of the second Thomson-scattering diagnostic was chosen to measure light scattered from SBS-driven ion-acoustic waves (Fig. 1d) that are excited by the SBS instability ($\mathbf{k} = \mathbf{k}_{||}$) [5].

The interaction beam was timed to turn on 1.0 ns after the heater beam. The 180 ps Gaussian Thomson probe beam was turned on 400 ps after the interaction beam near the peak of the backscattered SBS light .

The plasma has been well-characterized; Fig. 2a shows a constant electron temperature profile ($T_e = 450$ eV) along the interaction beam axis. The location of the Thomson-scattering volume and the focus of the interaction beam remained at TCC throughout the experiment; the target (and the heater beam) was moved to probe different positions in the plasma parallel to, and 400 μm from, the surface of the target.

Figure 2b shows a Thomson-scattering spectrum taken from the streak data in Fig. 1b. Two peaks corresponding to ion-acoustic fluctuations propagating along the direction of $\mathbf{k}_\perp$ are evident. Fitting the data using a standard theoretical form factor [6] gives the electron temperature. The measured peaks are broadened by velocity gradients perpendicular to the interaction beam. This broadening is to be expected as the initial plasma length is only y= 100 μm in the perpendicular direction; this Thomson-scattering diagnostic probes the plasma expanding in the perpendicular direction. The measured width of the peaks ($\delta\lambda$) gives an estimated velocity range $\frac{\delta v}{v}\left(\propto \frac{\delta\lambda}{\lambda}\right) = 0.5$ within the Thomson-scattering volume.

The blue-shifted intensity peak in the spectra mesured by the second Thomson-scattering diagnostic is a direct measure of the local resonant frequency of the ion-acoustic waves in the laboratory frame ($-\mathbf{k}_{||}$). The frequency of the scattered light in the laboratory frame is shifted from the laser frequency in two ways: by the frequency of the probed ion-acoustic wave (function of the electron temperature), and by the overall flow of the plasma relative to the frame of the laboratory (Doppler shift along $k_{||}$). Since the electron temperature is known, the plasma flow parallel to the z-axis is determined from the local frequency shift between the frequency of the Thomson-scattering probe ($\lambda_{3\omega} = 351.3$ nm) and the blue-shifted intensity peak.

Figure 2c shows a Thomson-scattering spectra in which two intensity peaks can be observed. The blue-shifted intensity peak is fit using the independently measured electron temperature, and a flow of $\frac{v}{c_s} = 0.7$ is measured. Note that the use of two Thomson-scattering diagnostics is necessary as the SBS-driven acoustic wave is not assumed to be at the local resonant ion-acoustic frequency. This is evident in Fig. 2c, where the red-shifted intensity peak and the corresponding resonant intensity peak are offset by 1.1 Å.

Figure 3d shows the plasma flow along the z-axis measured from the frequency of the local resonant ion-acoustic fluctuations ($-\mathbf{k}_{||}$). A 200 μm velocity plateau is measured in the center of the plasma; a Mach 1 flow was measured in the front edge of the plasma. One can directly observe the effect of the velocity gradient on SBS from the frequency mismatch between the measured frequency of the SBS driven acoustic wave, and the measured frequency of the local resonant waves.

Figure 3 shows spectra for representative data shots at three positions in the plasma; the frequency of the driven ion-acoustic wave remains unchanged ($\lambda = 3515$ Å) while the frequency of the local resonant ion-acoustic waves ($-\mathbf{k}_{||}$) increase as one moves from the plateau to the front of the plasma (this increase is a direct effect of the plasma flow as the electron temperature is constant). SBS light is scattered from the velocity plateau where large resonant acoustic waves are driven. The light scattered from the plateau and the incident light create a constant pon-

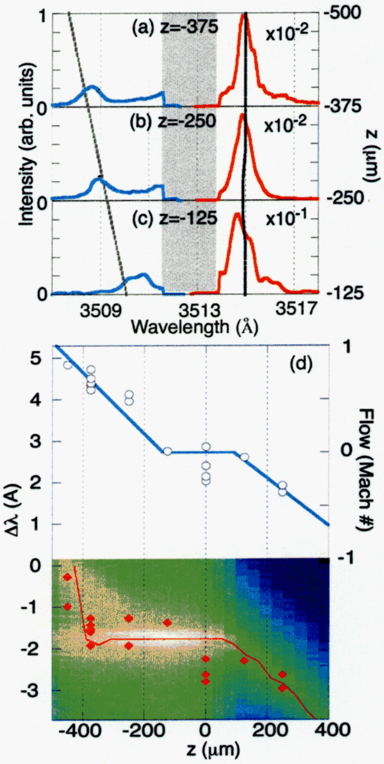

FIG. 3: Intensity spectra at z= (a) -375 μm, (b) -250 μm, and (c) -125 μm show a velocity gradient. Furthermore, the frequency of the SBS driven ion-acoustic wave is unchanged. The shaded area has been filtered by a factor of 10. (d) The wavelength shift for red-shifted (solid squares) and the blue-shifted (open circles) intensity peaks are plotted. The blue-shifted intensity peaks reveal a Mach 1 flow parallel to the interaction beam (right axis). A pF3d simulation is shown where large acoustic waves (color scale = δn/n$_e$) are driven in the plateau region.

deromotive force with a constant frequency profile in the front of the plasma. This constant frequency ponderomotive force drives non-resonant acoustic waves (i.e., the velocity gradient shifts the resonant frequency from the constant frequency of the ponderomotive force).

The experiment was simulated in 2-D using pF3d [7]. A $f/6$ RPP beam with a best focus of 60 μm and an average vacuum intensity of 10^{15} W cm^{-2} was propagated through a 1000 μm slab of plasma ($T_e = 450$ eV, $n_e = 1 \times 10^{20}$ cm^{-3}). A Mach 2 transverse flow (lateral expansion of the target) and the measured velocity profile along the propagation axis shown in Fig. 3d were included.

Figure 4a shows a plot of the interaction beam 70 ps into the simulation. Intensity of the most intense speckles is around 4×10^{15} W cm^{-2}. A linear non-local heat transport model was used, but had only a small effect on the results. The maximum local temperature fluctuation observed was $\frac{\Delta T}{T} \approx 30\%$ in the most intense speckles. The transverse flow suppressed most of the filamentation

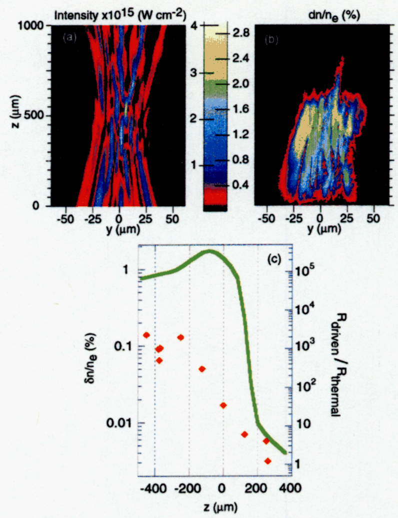

FIG. 4: (a) The intensity of the interaction beam is plotted 70 ps into the pF3d simulation. (b) The ion-acoustic waves are large in the front of the plasma. (c) The measured amplitude of the excited ion-acoustic wave (squares) is plotted as a function of the position along the interaction beam. The amplitude profile given by pF3d is also plotted (solid).

and the simulations show little beam bending (Fig. 4a).

Figure 4b and the solid line in Fig. 4c show that large ion-acoustic waves are driven by SBS only in the front half of the plasma [8]. The velocity gradient in the back of the plasma prevents any significant SBS growth. The plateau in the middle provides a resonant region where SBS drives a large acoustic wave. The amplitude of the driven acoustic wave saturates near the front of the velocity plateau. In the front of the plasma, the strong velocity gradient prevents SBS growth at the local resonant frequency but the reflected light coming from the plateau and the incoming light provide a constant frequency ponderomotive force that drives non-resonant acoustic waves. The off-resonant acoustic waves are clearly observed in Fig 3d. As one moves away from the plateau and towards the front of the plasma, the acoustic wave amplitude slightly decreases as the ponderomotive driver is increasingly off-resonance (Fig. 4c).

While the amplitude of driven acoustic waves ($\frac{\delta n}{n_e}$) is readily obtained from simulations, it has to be calculated from the intensity peaks in the Thomson-scattering spectra. This is done by comparing the scattered reflectivity from thermal fluctuations (i.e. the power scattered in to the left intensity peak in Fig. 2c divided by the incident laser power), which is given by:

$$R_{thermal} = \frac{1}{4} r_0^2 n_e L \Delta\Omega_{exp}$$

where r_0 is the classical electron radius, L is the length along the direction of the 3ω probe beam, and $\Delta\Omega_{exp}$ is the solid angle of the collecting optics (an f/5 lens), with the reflectivity scattered by the driven acoustic wave

UCRL-WEB-146893 Rev1-v4no1-03

given by:

$$R_{driven} = \frac{1}{4} r_0^2 n_e^2 \lambda_{3\omega}^2 L L_c (\delta n/n_e)^2$$

where $\delta n/n_e$ is the amplitude of the acoustic wave and L_c its correlation length along the direction of the 3ω probe beam. L_c can be estimated by the transverse size of speckles generated by the interaction beam $f_{2\omega}\lambda_{2\omega}$.

Figure 4c shows that this estimation of $\delta n/n_e$ reproduces the overall spatial shape predicted by pF3d, but the absolute amplitude is smaller by almost an order of magnitude. Various factors can explain this discrepancy. For instance, any misalignment of the optics, an overestimation of L_c, or enhanced thermal fluctuations would lead to an underestimation of the acoustic wave amplitude. Assuming the latter, we have verified that increasing the amplitude of the thermal noise source used both in the Thomson-scattering calculations and in the SBS simulations by an order of magnitude gives a good agreement between the measured and simulated wave amplitude and spatial profiles. A study of the amplitude of the thermal noise in laser plasmas needs to be completed to investigate the discrepancies in the calculated wave amplitudes seen in this and other studies [9].

The effect of detuning SBS by a velocity gradient is further verified by post processing the simulation providing a measure of the local frequency of the driven ion-acoustic waves. This agrees well with the experimentally measured frequencies, as shown in Fig. 3d; off-resonant driven ion-acoustic waves are evident in the front part of the plasma.

A peak SBS reflectivity of 6% was measured. The SBS spectrum (Fig. 5) confirms our analysis of the effect of the velocity gradient on SBS. The frequency of the peak intensity is consistent with the frequency of the large off-resonant waves observed by Thomson scattering in the front part of the plasma, and corresponds to the resonant acoustic frequency in the velocity plateau. The spectrum has a tail towards the fundamental frequency that corresponds to light scattered from the flow propagating towards the detector. There is a sharp cutoff towards higher wavelengths indicating that there is no scattering coming from the back of the plasma where the velocity flow is propagating away from the detector. This is consistent with the fact that we measure very small ion-acoustic waves in the back portion of the plasma (Fig. 4c). Overall, the SBS spectrum is characteristic of the central plateau, while the expanding plasma only slightly modifies its shape.

In summary, we have presented the first direct measurement of SBS detuning by a velocity gradient. We studied an expanding plasma with a central velocity plateau. The frequency mismatch between the frequency of the SBS driven ion-acoustic wave and the local resonant frequency (as measured from thermal waves) was mapped throughout the plasma. It was found that acoustic waves in the flow are driven off-resonance by the ponderomotive force with a beat frequency created by the incoming light and the light reflected from the plateau. This detuning inhibits further SBS growth in the flow. These findings are important to many laser-plasma experiments and occurs in various ICF direct drive [10] and indirect drive targets [9]. We have shown that the SBS spectrum gives insight into the locations of SBS growth, and Thomson scattering on driven ion-acoustic waves provides a direct verification of modeling the effect of a velocity gradient on SBS.

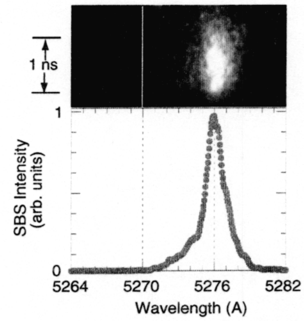

FIG. 5: Ths SBS spectra is plotted as a function of intensity. The peak intensity corresponds to light scattered from the velocity plateau; a tail towards the fundamental frequency corresponds to light scattered from ion-acoustic waves in the front of the plasma.

We would like to acknowledge the efforts of the Trident laser crew: R. Johnson, T. Hurry, R. Gonzales, N. Okamoto, F. Archuleta and R. Perea in target fabrication. We thank D. Montgomery, and H. Baldis for valuable discussions. We further thank R. Scalettar and the UC Davis Physics Department for their support. This work was performed under the auspices of the U.S. Department of Energy by the Lawrence Livermore National Laboratory under Contract No. W-7405-ENG-48.

---

* Also at Physics Department, University of California at Davis, 95616.

[1] C. S. Lui et al., Physical Review Letters **31** (1973).
[2] N. K. Moncur et al., Applied Optics **34**, 4274 (1995).
[3] B. S. Bauer et al., Physical Review Letters **74**, 3604 (1995).
[4] D. H. Froula et al., Physics of Plasmas **9** (2002).
[5] D. H. Froula et al., Physical Review Letters **88**, 105003 (2002).
[6] D. E. Evans, Plasma Physics **12**, 573 (1970).
[7] R. L. Berger et al., Physics of Plasmas **5**, 4337 (1998).
[8] J. A. Cobble et al., Physics of Plasmas **7**, 323 (2000).
[9] S. H. Glenzer et al., Physical Review Letters **77**, 1496 (1996).
[10] W. Seka et al., Physical Review Letters **89**, 175002 (2002).